

# CMS Internal Note

*The content of this note is intended for CMS internal use and distribution only*

---

**April 2003**

## Hard diffractive scattering at LHC energies

A. Godizov, V. Petrov, A. Prokudin, R. Ryutin

*Institute for High Energy Physics, Protvino, Russia*

***IHEP Study Group on Elastic and Diffractive Scattering at LHC***

### **Abstract**

Some first results on Higgs boson and dijet diffractive production are presented. The study of the diffractive pattern needs combined CMS-TOTEM (or other low- $t$  facility) measurements.

# 1 Introduction

Experiments at the LHC which aim to study low- (TOTEM, ...) and high- (CMS, ...)  $p_T$  regimes, related to typical undulatory (diffractive) and corpuscular (point-like) behaviour of the corresponding cross sections, may offer a very exciting possibility to observe an interplay of both regimes [1]. In theory the "hard part" can be (hopefully) treated with perturbative methods while the "soft" part is definitely nonperturbative.

Below we give two examples of such an interplay: exclusive Higgs boson production by diffractively scattered protons and exclusive production of two gluon jets.

Both processes are related to the same dominant amplitude of exclusive two-gluon production. The driving mechanism of the diffractive processes is the Pomeron. Data on the total cross section demands unambiguously for a Pomeron with larger-than-one intercept, and thus the need of "unitarization" to avoid the contradiction to the basic principle of S-matrix unitarity in quantum field theory. The direct consequence of this principle is the Froissart-Martin bound [2]

$$\sigma_{tot}^{hh}(s) \leq \frac{\pi}{m_\pi^2} \ln^2(s/s_0), s \rightarrow \infty. \quad (1)$$

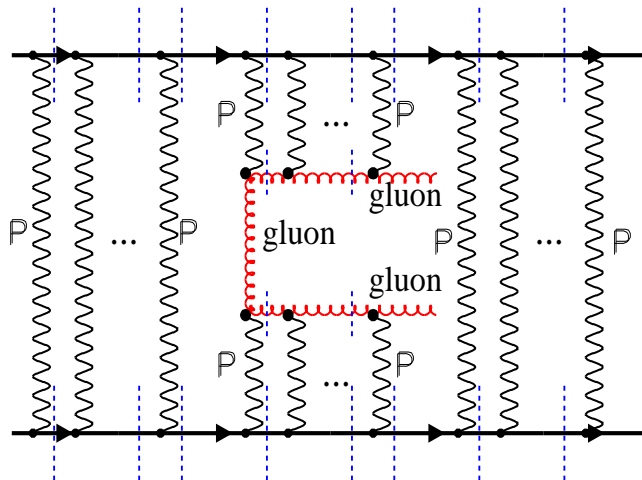


Figure 1: The full unitarization of the process  $p + p \rightarrow p + gluon + gluon + p$

In Fig. 1 we depict as an example a diagram of the corresponding Pomeron exchanges for the process  $p + p \rightarrow p + gluon + gluon + p$ . On-shell proton-proton amplitudes and off-shell proton-gluon amplitudes are treated by the method developed in Ref. [3], which is based on the extension of the Regge-eikonal approach, and successfully used for the description of the HERA data on the exclusive vector meson production [4]. Simple Regge description of the above process is depicted in Fig. 2. Usually it is called Double Pomeron Exchange (DPE). Since the effect of the unitarity violation in DPE is rather large at LHC energies, it is better to use the improved Regge-eikonal approach ("unitarized DPE"). Amplitude in this approach is the infinite sum of all possible Pomeron exchanges.

## 2 Diffractive Higgs boson production

The amplitude of the process  $p + p \rightarrow p + H + p$  consists of two parts (see Fig. 3). The "hard" part  $F$  is the usual gluon-gluon fusion process calculated in the Standard Model[5]. The "Soft" amplitudes  $T_{1,2}$  are parametrized according to the extended Regge-eikonal approach [4].

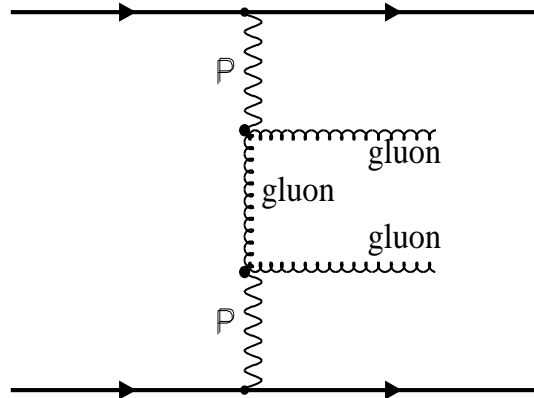


Figure 2: Usual DPE approach to the process  $p + p \rightarrow p + gluon + gluon + p$

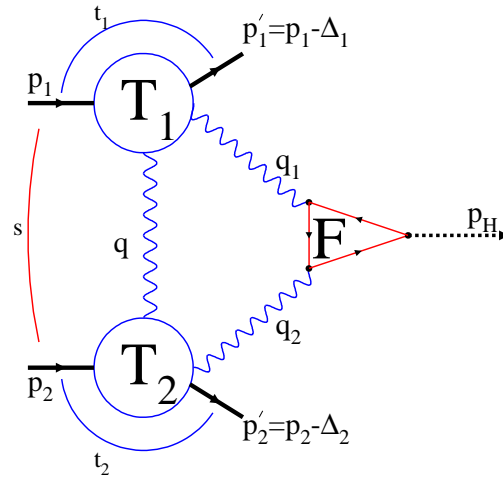


Figure 3: The process  $p + p \rightarrow p + H + p$ . The absorption in the initial and final pp-channels is not shown.

We use the following kinematical cuts

$$0.03 \text{ GeV}^2 \leq |t_{1,2}| \leq 1 \text{ GeV}^2, \quad (2)$$

$$\xi_{Min} \simeq \frac{M_H^2}{s\xi_{Max}} \leq \xi_{1,2} \leq \xi_{Max} = 0.1, \quad (3)$$

that correspond to the double Regge limit and the existence of two rapidity gaps. Here  $\xi_{1,2}$  are momentum fractions carried by gluons, and  $t_{1,2}$  are momentum transfers squared of protons, as indicated in Fig. 3. For the above kinematics final protons have large rapidities,  $y_p > 9$ , thereof the need to have combined CMS and low- $t$  measurements via roman pots to use the missing mass method.

The first result of our calculations is the normalized  $t$  distributions  $w(t) = d\sigma/dt/\sigma_{tot}$  (see Fig. 4) for LHC and Tevatron. The shrinkage of the diffraction peak with decreasing Higgs boson mass is a direct consequence of the existence of the additional hard scale  $M_H$ . It leads to changes in the shape and size of the interaction region.

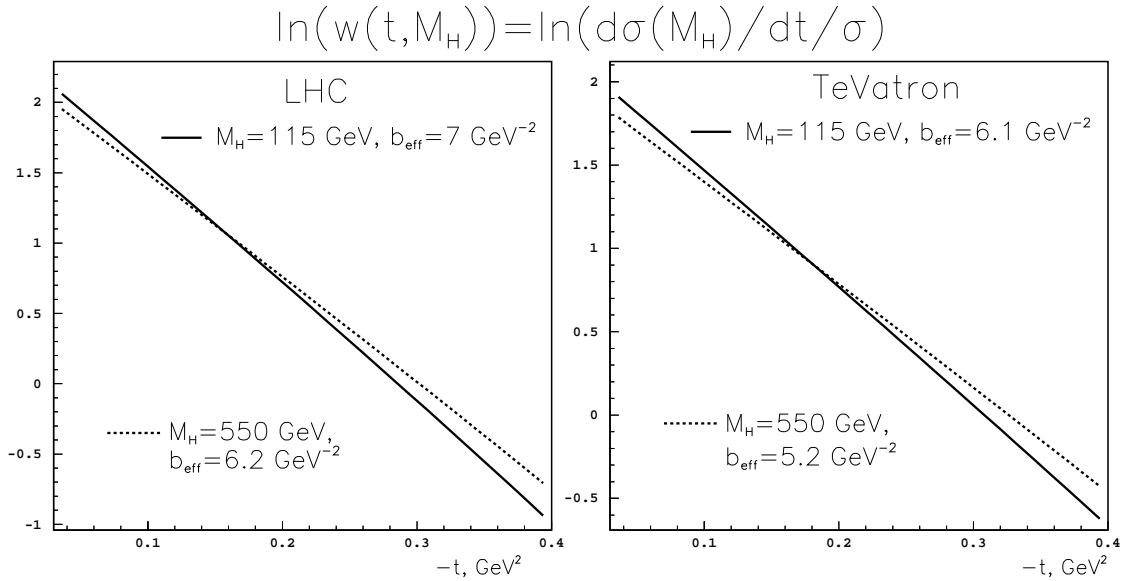


Figure 4: Differential cross section of the process  $p + p \rightarrow p + H + p$  for two values of the Higgs boson mass.

The second result is the total cross section versus the Higgs boson mass. The values of the cross section are about  $70 \div 150$  fb in the interval of Higgs boson masses from  $M_H = 100$  GeV to  $M_H = 300$  GeV (see Fig. 5). The form of the curve originates from the standard gluon-gluon-Higgs boson vertex and has a peak near  $M_H \simeq 2m_t$ . For  $M_H = 115$  GeV at LHC we have a lower bound of  $\sigma_{tot} \simeq 70$  fb for the cross section. It is instructive to compare our result with other studies. The most pessimistic one is the result of Ref. [6], where the value of the total cross section is about 5.7 fb. The origin of this small value is the multiplication by a survival probability factor that strongly reduces the cross section. Another reason is that we use a fully nonfactorized form of the amplitude [7]. It takes into account all the effects of internal gluon loop integration and tensor structure of proton-gluon vertices. A more optimistic result is given in [8], where a cross section 200 fb for  $M_H = 100$  GeV at LHC energies was obtained. They used also a nonfactorized form of the amplitude and a QCD inspired model for  $g^*p \rightarrow g^*p$  amplitudes, taking into account the nonperturbative proton wave functions. Our model is based on the parametrization [4] of the Regge-eikonal approach for  $g^*p \rightarrow g^*p$  amplitudes, which is primordially nonperturbative and normalized to the data from HERA on  $\gamma p \rightarrow Vp$  scattering. To obtain all the parameters we use the representation for the vector meson production amplitude, which is depicted in Fig. 6, where the quark box is calculated in QCD. It is important to note, that all the predictions depend on the theoretical interpretation of the available experimental data. Thus we can only estimate the result within different scenarios.

To estimate the signal to QCD background ratio for  $b\bar{b}$  signal we assume:

- The possibility to separate final  $b\bar{b}$  quark jets from gluon jets. If we can not do it, it will increase the background by two orders of magnitude under the 50% efficiency.

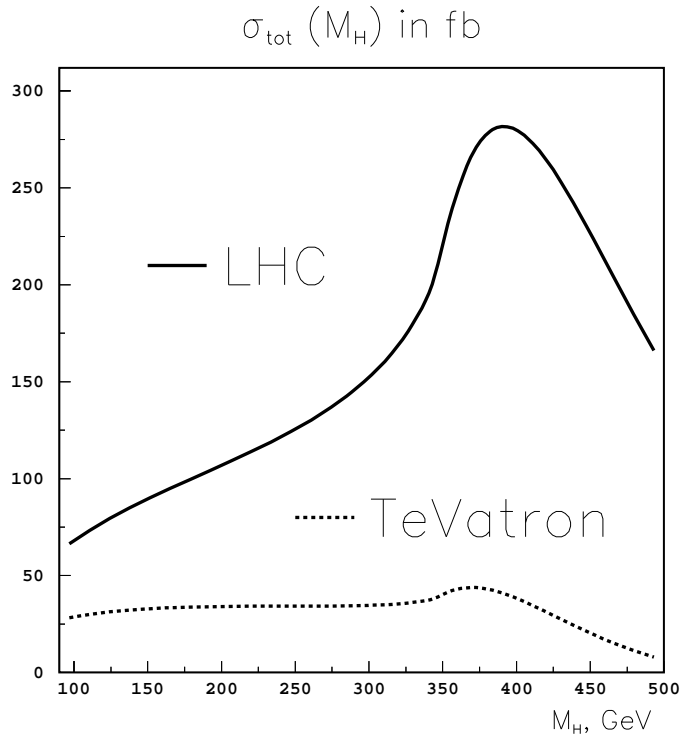


Figure 5: The total cross section of the process  $p + p \rightarrow p + H + p$  versus Higgs boson mass

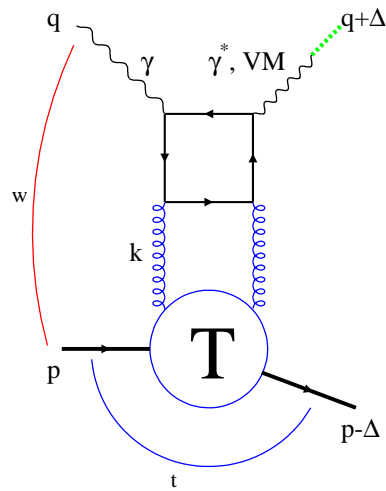


Figure 6: The process  $\gamma + p \rightarrow V + p$ .

- A suppression due to the absence of colour-octet  $b\bar{b}$  final states
- A suppression of light fermion pair production, when  $J_{z,tot} = 0$
- A cut  $E_T > 50 \text{ GeV}$  ( $\theta \geq 60^\circ$ ), since the cross section of diffractive  $b\bar{b}$  jet production strongly decreases with  $E_T$ .

The preliminary result of these estimations is

$$\begin{aligned} \frac{Signal(pp \rightarrow pHp \rightarrow pb\bar{b}p)}{QCD \ background} &\geq \\ &\geq 9.5 \cdot 10^{-6} |A|^2 Br_{H \rightarrow Q\bar{Q}} \frac{M_H^3}{\Delta M}, \end{aligned} \quad (4)$$

where  $|A|^2 \simeq 0.5 \div 3$  for Higgs boson masses  $100 \div 350 \text{ GeV}$ . For  $M_H \simeq 115 \text{ GeV}$

$$\frac{Signal(pp \rightarrow pHp \rightarrow pb\bar{b}p)}{QCD \ background} \geq 3.8 \frac{GeV}{\Delta M}, \quad (5)$$

where  $\Delta M$  is the mass resolution of the detector. The result does not differ much from results of other authors. Therefore we conclude that the hard part of the amplitude plays the main role in these estimations.

Hence there is a possibility to detect the Higgs boson using the usual  $b\bar{b}$  decay mode for a luminosity larger than  $10 \text{ fb}^{-1}$ . We could stop at this point and solve the only problem: Higgs boson detection. But we could use all the advantages of the exclusive process to reconstruct the whole event of Higgs boson production via missing mass measurements, and also for the investigation of the diffractive pattern of the interaction.

### 3 Hard Diffractive pattern at LHC

In diffractive processes some short-time vacuum fluctuations can lead to the production of hard partons, observed as hadronic jets. In our opinion a problem of great experimental and theoretical interest is to find out how does this diffraction picture change with the presence of jets and with changing kinematics of the jets. We suppose that the main contribution to the diffractive exclusive dijet production processes is given by subprocesses like the one on Fig. 7

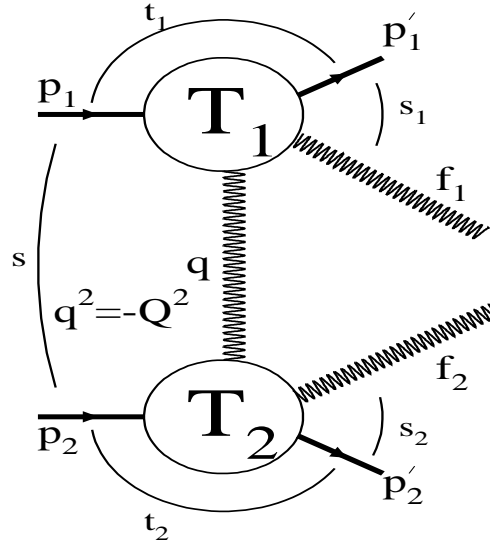


Figure 7: The process  $p + p \rightarrow p + jet + jet + p$ . The absorption in the initial and final pp-channels is not shown.

In fact, in double diffractive processes the initial proton is not scattered by the other proton but by hard vacuum fluctuations. For the calculation of the invariant amplitudes for unitarized double pomeron exchange we use the

phenomenological non-perturbative Regge-eikonal model. This model is based on the general principles of the quantum field theory such as the S-matrix unitarity extended to off-shell amplitudes [3].

Unfortunately, at present we do not have enough experimental data to normalize the exclusive dijet production cross section. So we present only average values, ratios and normalized distributions in the following kinematical range:

$$\sqrt{s} = 14(1.8) \text{ TeV} , |t_{1,2}| \leq 1 \text{ GeV}^2 , \xi_{1,2} \leq 0.1 , E_{T1,2} \geq 7 \text{ GeV} . \quad (6)$$

In the Fig. 8 the normalized  $t$  distribution is shown. The slope of the curve changes slightly from Tevatron to LHC energies. This fact can be explained by the presence of hard virtual gluon scale.

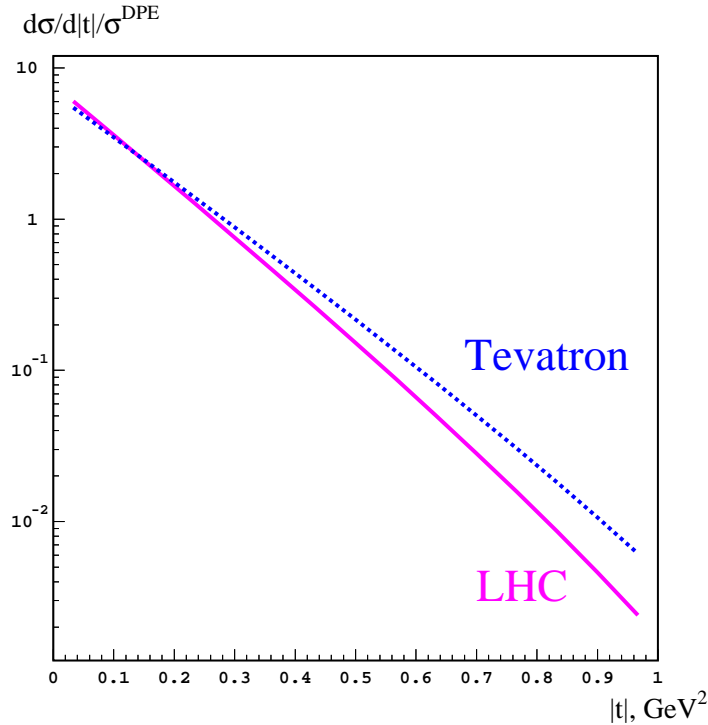


Figure 8: The  $t$  distribution.

The  $E_T$ -distribution curve (Fig. 9) has a very strong powerlike decreasing behaviour. As a consequence we have a strong dependence of the DPE cross section on the  $E_T$  cut in the above kinematical range. The change in the transverse energy cut from 7 to 10 GeV reduce the DPE cross section by a factor 10.

In Fig. 10 the  $\xi$ -distribution is depicted and we can see that the contribution of events with small  $\xi$  to the DPE cross section is much larger at LHC than at Tevatron.

The different behaviour of the curves at extra small  $\xi$  values can be explained by the natural kinematical restriction

$$E_T^2 < \frac{\xi_1 \xi_2 s}{4} . \quad (7)$$

It implies that the jet transverse energy squared has to be less than one fourth of the dijet invariant mass.

At the end we present values of the proton transferred momentum squared module, proton lost energy fraction and jet transverse energy averaged over the considered kinematical range

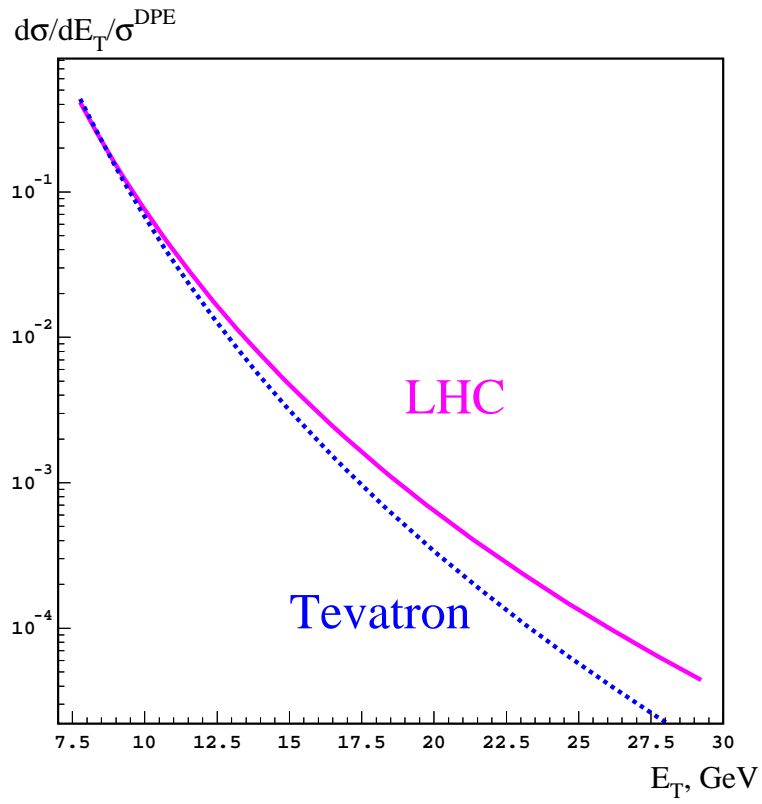


Figure 9: The  $E_T$ -distribution.

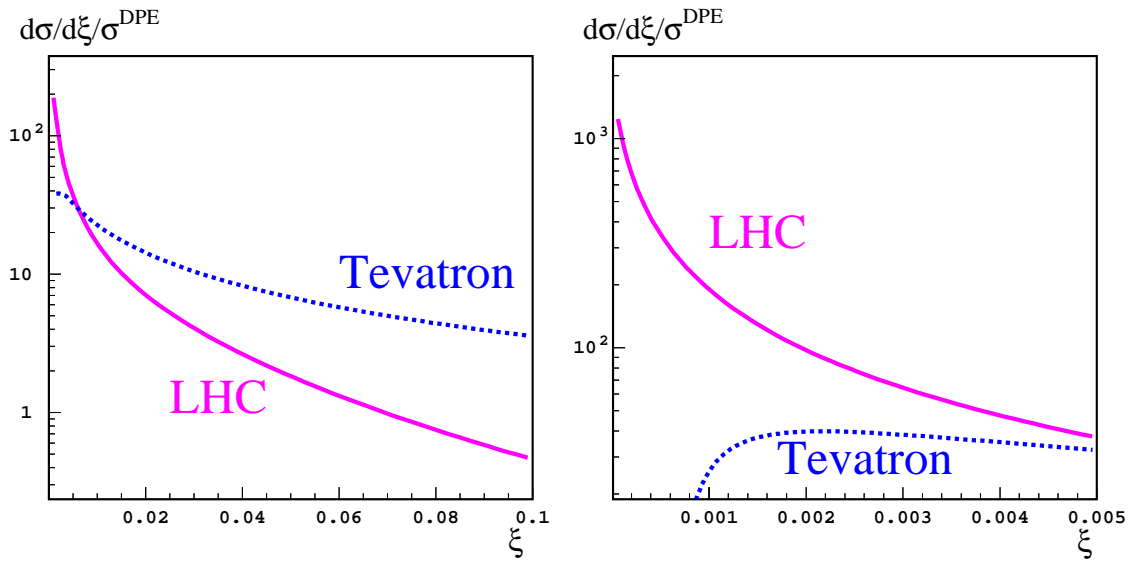


Figure 10: The  $\xi$ -distribution.



$$\begin{aligned}
& \underline{Tevatron(\sqrt{s} = 1.8 \text{ TeV})} : \quad \underline{LHC(\sqrt{s} = 14 \text{ TeV})} : \\
& \langle |t| \rangle \simeq 0.145 \text{ GeV}^2 , \quad \langle |t| \rangle \simeq 0.125 \text{ GeV}^2 , \\
& \langle \xi \rangle \simeq 0.03 , \quad \langle \xi \rangle \simeq 0.01 , \\
& \langle E_T \rangle \simeq 8.4 \text{ GeV} , \quad \langle E_T \rangle \simeq 9.0 \text{ GeV} ,
\end{aligned} \tag{8}$$

and ratios for DPE cross sections at different energies and  $E_T$  cuts

$$\begin{aligned}
& \frac{\sigma_{Tevatron}^{DPE}(E_T > 10 \text{ GeV})}{\sigma_{Tevatron}^{DPE}(E_T > 7 \text{ GeV})} \simeq 0.1 , \\
& \frac{\sigma_{LHC}^{DPE}(E_T > 10 \text{ GeV})}{\sigma_{LHC}^{DPE}(E_T > 7 \text{ GeV})} \simeq 0.14 , \\
& \frac{\sigma_{LHC}^{DPE}(E_T > 7 \text{ GeV})}{\sigma_{Tevatron}^{DPE}(E_T > 7 \text{ GeV})} \simeq 2.7 , \\
& \frac{\sigma_{LHC}^{DPE}(E_T > 10 \text{ GeV})}{\sigma_{Tevatron}^{DPE}(E_T > 10 \text{ GeV})} \simeq 3.7 .
\end{aligned}$$

In [9] authors set an upper bound for DPE cross section at  $\sqrt{s} = 1.8 \text{ TeV}$  in the kinematical range

$$0.035 < \xi_{\bar{p}} < 0.095 , \quad 0.01 < \xi_p < 0.03 , \quad E_T > 7 \text{ GeV} , \quad -4.2 < \eta < 2.4 .$$

to be 3.7 nb.

Using this value we can obtain the upper bound  $\sigma_{LHC}^{DPE} < 100 \text{ nb}$  for the cross section at LHC in the range (6).

## 4 Conclusions

We observe that the study of the hard diffraction processes is of great interest and can exhibit quite peculiar features. It is the real possibility to find Higgs boson and other particles in the exclusive double diffractive process, since cross sections are rather large and background is suppressed. Diffractive properties of the scattering amplitudes at very high energy can be investigated, that's why we propose to use combined CMS and low- $t$  measurements.

More detailed results will be presented elsewhere. We would like to acknowledge A. De Roeck for his useful corrections and comments. We thank participants of the 2002 December CMS Week for interesting and suggestive discussions.

## References

- [1] V.A. Petrov, A.V. Prokudin, S.M. Troshin, N.E. Tyurin, *J. Phys. G: Nucl. Part. Phys.* 27 (2001) 2225.
- [2] A. Martin, *Phys. Rev. D* 129 (1963) 993;  
M. Froissart, *Phys. Rev. D* 123 (1961) 1053.
- [3] V.A. Petrov, *Proceedings of the VIIth Blois Workshop* (Ed. M. Haguenaer et al., Editions Frontieres; Paris 1995).
- [4] V.A. Petrov and A.V. Prokudin, *Phys. Atom. Nucl.* 62 (1999) 1562.; hep-ph/9912245
- [5] A. Kniehl, *Phys. Rept.* 240 (1994) 211.
- [6] V. A. Khoze, A. D. Martin and M. G. Ryskin, *Eur. Phys. J. C* 14 (2000) 525.
- [7] A. Berera, J. C. Collins, *Nucl. Phys. B* 474 (1996) 183.
- [8] J.-R. Cudell and O. F. Hernandez, *Nucl. Phys. B* 471 (1996) 471.
- [9] **CDF Collaboration**, T. Affolder et al., *Phys. Rev. Lett.* 85 (2000) 4215.